

# Metamaterials: An Enabling Technology for Wireless Communications

Omar M. Ramahi, Muhammad S. Boybay, Omar Siddiqui, Leila Yousefi, Ali Kabiri, Hussein Attia, Mohammad Bait-Suwailam and Zhao Ren

<sup>1</sup>Electrical and Computer Engineering Department, University of Waterloo, Waterloo, Ontario, N2L 3G1, Canada

**Keywords:** Metamaterials, Wireless Communication

**Abstract.** Metamaterials are structures that provide electromagnetic properties not found in naturally occurring media; properties such as negative index of refraction, negative permittivity, or negative permeability. Since the appearance of Pendry's seminal work in the year 2000 on the feasibility of creating material with negative refractive index, a deluge of papers were published on metamaterials proposing the existence of phenomena and applications never conceived before. So why would such excitement about something that was not intended to be present naturally? The answer is simple. We tend to design or envision applications based on what we believe to exist. It is fair to argue that many applications were not envisioned simply because they would have to be based on materials that do not exist. With the realization of metamaterials, new phenomena and applications became not only possible, but even practical. In this paper, we discuss metamaterial applications that our group at the University of Waterloo has focused on. These applications are mostly related to wireless communication systems including sensing.

## I. Introduction

Metamaterials are in essence electrically-small resonators. A structure that is electrically small implies that the size of the structure is much smaller than the wavelength in free space. The resonance that takes place in these structures is the result of an applied field that generates either a magnetic dipole moment, electric dipole moment or both in the small resonators. This resonance phenomenon is in sharp contrast to the constructive interference between waves bouncing back and forth along or within a traditional resonator such as a transmission line or cavity. For instance, in the artificial magnetic material type of metamaterials, the frequency range of interest will be immediately before the resonance frequency, whereas for single-negative type of metamaterials, the interest would be in the frequency range immediately above resonance.

In addition to providing enhanced magnetic or dielectric properties, metamaterials are fundamentally dispersive due to the inherent laws of physics governing the magnetization and polarization of materials or structures. So the question arises as to how such new interesting structures with properties not found in naturally available material provide engineering value, especially in the area of wireless communications? Here, the definition of wireless communications embodies hardware such as transmitters, receivers, antennas used for point-to-point communications, devices for RF, microwave, THz and optical frequencies transmission, and devices used for non-invasive detection or monitoring.

While metamaterial have seen applications in wide area of engineering disciplines, here, we focus on engineering applications related to the important area of wireless communications. We address how metamaterial can have a strong impact on the performance of planar antennas, Multi-Input Multi-Output antenna systems, electromagnetic interference in printed circuit boards and packages, microwave non-invasive detection using near-field microscopy, and, finally, biosensing.

## II. Gain Enhancement of Antennas

The Gain of the antenna is one of its most important characteristics. The higher the gain of the antenna, the more energy the antenna send in a specific direction. The efficiency, another critical antenna performance parameter, is a measure of how much energy the antenna radiates in comparison to the energy that it receives. While there are many techniques to enhance these two important characteristics, keeping the antenna size within specific size, or footprint, remains a formidable challenge. Here, we discuss an application of metamaterials where planar antennas are considered.

Metamaterial has been used previously to minimize surface waves arising from microstrip patch antennas. Here, our objective is to increase the gain of the microstrip antenna while maintaining its low attractive low profile feature. Traditionally, when non-magnetic superstrates are used for gain enhancement, the thickness of the superstrate is typically close to half of the wavelength in the media (Jackson, 1985). Using magneto-dielectric materials as the superstrate decreases the wavelength in the media leading to a lower profile. Furthermore, we expect a significant reduction in surface waves if the proper type of metamaterials' inclusions is used. Previous trends to enhance the gain of planar antennas include the use of non-magnetic dielectric

(Jackson, 1985) or electromagnetic bandgap structures (Attia, 2008, Lee, 2005) as a superstrate. However, all these trends require fairly thick layers, leading to an unattractive increase in the antenna profile.

In this work, a novel engineered magnetic superstrate using modified split ring resonator (MSRR) inclusions is employed. The MSRR unit cell is designed to have *positive* values for the effective permeability and permittivity at the resonance frequency of the antenna. The MSRR inclusion used here consists of two parallel broken square loops as shown in Fig. 1(a). (The host dielectric is Rogers RO4350 with a thickness of 0.762 mm, relative permittivity of  $\epsilon_r = 3.48$ , and loss tangent of  $\tan\delta = 0.004$ .) A planar 10 X 10 array of MSRRs was printed on the host dielectric layer to provide the engineered magnetic material. The superstrate used here consists of 3 layers of printed magnetic inclusions. The layers are separated by 2 mm of air layers (see Fig. 1(b)).

The patch antenna used here has dimensions of 36 mm x 36 mm, and is printed on a substrate of the same characteristics and dimensions as used for the MSRR. The antenna is designed to operate at the frequency band of 2190-2210 MHz (which is very close the downlink band of UMTS) at which the magnetic superstrate has an effective permeability of about 15 (real part) and a magnetic loss tangent of 0.11. Fig. 2(a) shows the return loss of the microstrip antenna before and after using the artificial magnetic superstrate at the optimized distance of 12 mm from the substrate. The overall profile of the structure is only  $\lambda_0/7$  where  $\lambda_0$  is the free-space wavelength at the resonance frequency. As shown in Fig. 2(a), the antenna impedance bandwidth ( $S_{11} < -10$  dB) and the resonance frequency of 2.2 GHz are practically unchanged when using the metamaterial superstrate in comparison to the case without superstrate. Fig. 2(b) shows the gain of the microstrip antenna before and after using the artificial magnetic superstrate. The gain is improved by 3.4 dB at the resonance frequency after using the engineered superstrate. More interestingly, the efficiency of the antenna at the operating frequency of 2.2GHz, has increased by 17% due to the metamaterial superstrate.

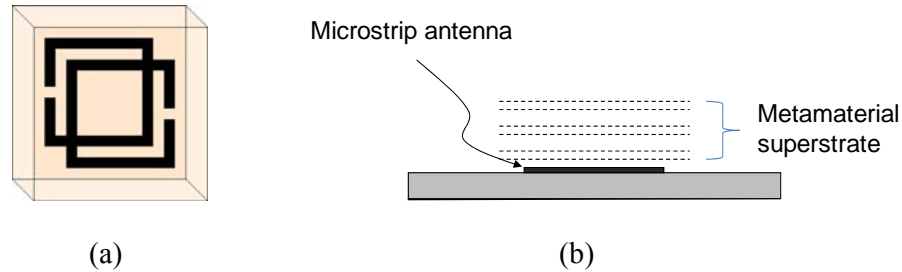


Fig. 1. (a) Modified Split Ring Resonator used to construct metamaterial. (b) A microstrip patch antenna with metamaterial superstrate.

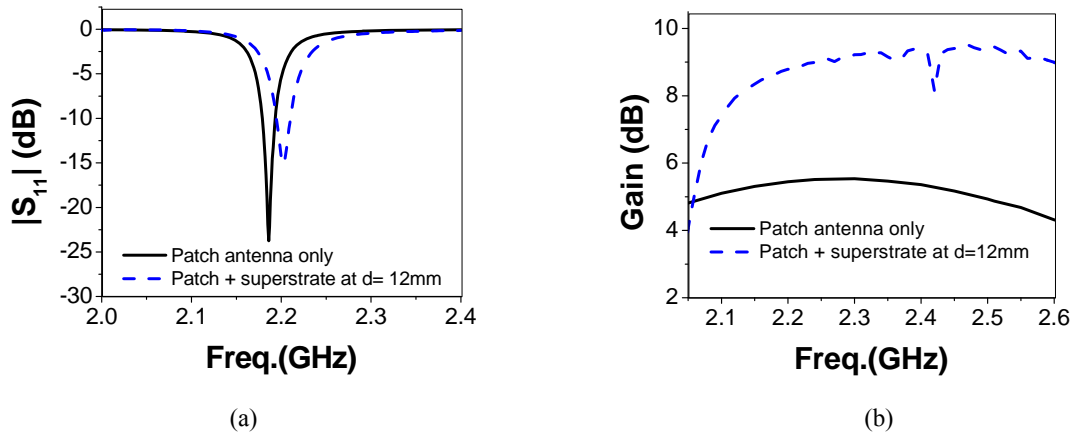


Fig. 2. (a) Magnitude of the return loss of the microstrip antenna before and after using the artificial magnetic superstrate. (b) The gain of the microstrip antenna before and after using the artificial magnetic superstrate for different distances between the antenna and superstrate.

### III. Electromagnetic Coupling Reduction in High-Profile Antennas using Single-Negative Metamaterials for MIMO Applications

It is known that the performance in antenna arrays in multiple-input multiple-output (MIMO) systems can be degraded when the antenna elements are in close proximity. The degradation is due to near-field effects, diffraction from finite-ground planes, strong inductive as well as capacitive coupling between the elements (Bhattacharyya, 1963). Higher degree of decorrelation leads to increasing the throughput and capacity of the antenna system.

The performance of MIMO antenna elements can be evaluated using the *envelope correlation* parameter, which can be derived from scattering parameters (Vaughan, 1987). Artificial magnetic inclusions, in the form of split-ring resonators, can have negative permeability values over a certain frequency band (Chen, 2008), (Dossche, 2005). Thus, the SNG materials is expected to block electromagnetic waves from propagation, if the external magnetic field is perpendicular to the openings of the SRR rings. If the split-ring resonators can function as insulator to block electromagnetic waves, then reduction in mutual coupling between the antenna elements can be achieved. Thus, the resonators behave like an insulator.

Fig. 3(a) shows the model setup used for the analysis considered in this work, comprising two closely spaced monopole antennas separated by a distance,  $d=\lambda/8$ , where  $\lambda$  is the wavelength of operation. The two antennas have been designed to resonate at a frequency of 1.24 GHz. A finite copper ground plane of size  $1.25\lambda \times 1.25\lambda$  is used. Stacks of SRR inclusions are aligned vertically between the two monopole antennas. The SRR inclusions are designed to have negative real permeability values around the same operational frequency as the antenna elements. The magnetic resonators considered here are rectangular split-ring resonators, with equal side lengths of 12 mm. The SRR rings with opposite cut openings are etched on the sides of a dielectric substrate with a thickness of 0.762 mm. The size of the dielectric substrate,  $L$ , is 16mm X 16 mm, which is much less than the operating wavelength. The SRR rings are made of copper with a thickness of 20  $\mu\text{m}$ . In this work, 4 SRR inclusion pairs are etched on both sides of the dielectric substrate. A total of 10 strips had been used in the measurement. Fig. 3(b) shows the fabricated prototype. The prototype system shown in Fig. 3 was fabricated using two brass rods of length 57 mm and diameter of 1.3 mm, fed by a 50  $\Omega$  coaxial cables. The scattering parameters are computed, and a two-antenna system with no spacer (Air case) is used as a reference for comparison purposes. Fig. 4 shows the measured magnitude of  $S_{11}$ , the measured mutual coupling,  $S_{21}$ , between the two antenna elements, and the correlation, all presented with and without the metamaterial inclusions placed between the two antennas.

By placing the SRR inclusions between the antennas, the mutual coupling,  $S_{21}$ , has been reduced by almost 20 dB at the resonance frequency, while at the same time maintaining good impedance matching for the two-antenna system from 1.1 GHz to 1.32 GHz. Furthermore, the envelope correlation,  $\rho_e$ , for the antenna system with SRR inclusions has improved significantly. Usually, a correlation of a minimum of -3 dB is considered sufficient for MIMO systems. The two-monopole antenna system with SRRs have an envelope correlation that is almost 40 dB better than the case in which SRRs were not used.

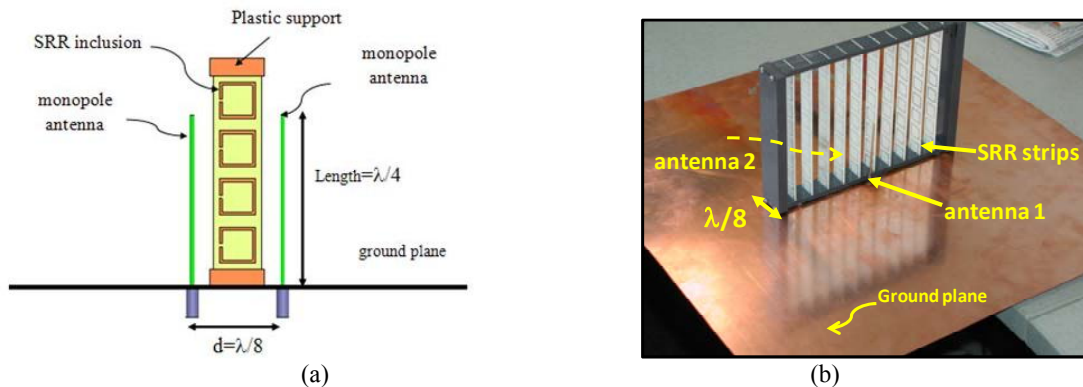


Fig. 3. (a) Schematic showing the insertion of metamaterial of the SRR type between two monopole antennas separated by only  $\lambda/8$ . (b) Fabricated structure.

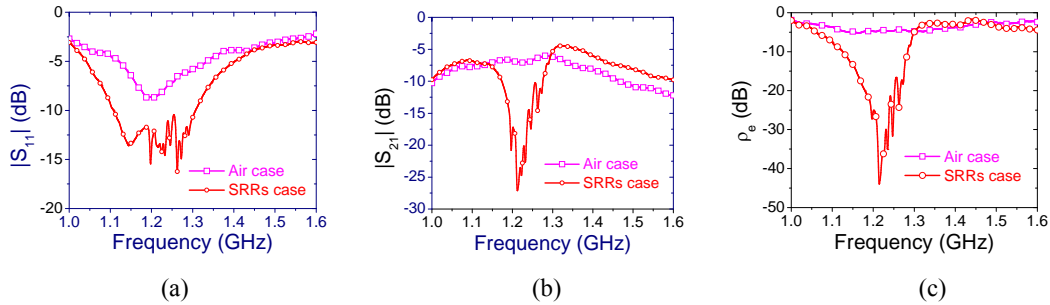


Fig. 4. (a) Magnitude of  $S_{11}$  corresponding to the impedance bandwidth of the antennas. (b) Magnitude of  $S_{21}$  corresponding to the coupling between the two antennas and (c) The correlation function.

#### IV. Metamaterial for Electromagnetic Noise Suppression

With the dramatic increase in clock frequency, demands for reduced noise margin and low voltage consumption, simultaneous switching noise (SSN) in multilayer printed circuit boards and packages that contain CMOS-based devices remains a severe challenge. With hundreds or more gates switching simultaneously within a power plane, SSN, if uncontrolled, can lead to false switching states in logic gates as well as degradation of the quality of signals transmission. Traditional trends for mitigating noise resonances rely on using decoupling capacitors between power planes. However, those discrete capacitors are limited in their noise mitigation capabilities, due to the lead inductance which cannot be eliminated. Recently, High-impedance surfaces or electromagnetic bandgap structures, have been introduced for noise suppression in printed circuit boards (Kamgaing, 2003), (Shahparnia, 2004). Although the bandgap structures are effective in terms of noise mitigation and signal integrity performance, they require an additional layer, thus adding to the overall cost. Moreover, conductive vias are needed for the embedded bandgap structures, thus incurring additional cost and fabrication requirements.

Planar bandgap structures have been introduced for noise isolation in mixed signal boards (Choi, 2004). SRRs and possibly other shapes resonate when an applied magnetic field is normal to their axis. This resonance behavior is due to the induced electromotive force that effectively induces current which flows within the metallic rings. This in turn gives an effective inductance which when balanced with the capacitive effect due to the capacitance between the rings and the cuts in the rings, gives rise to magnetic resonances. In other words, magnetic bandgap behavior is realized due to such excitation. By a dual principle based on the Babinet's principle (Falcone, 2004) *complementary* SRRs are expected to respond to an axial electric field when excited normally to the CSRRs axis. Thus, CSRRs possess an electrical resonance (or electrical bandgap behavior) upon an axial E-field excitation. Fig. 5(a) shows a split ring resonator unit cell with its complementary screen (CSRR). Interestingly, with the electric field being normal to the PCBs board, one can achieve a filtering behavior (i.e., bandgap) when such resonators are made part of the power plane structure.

To realize such filtering behavior, the CSRRs are etched in a single metallic layer. To achieve wide band filtering, we cascade several CSRR rings with different radii, placed concentrically as shown in Fig. 5(b). In fact, the resonances, or bandgaps (i.e., stop bands over which no transmission or energy transfer would cease upon an axial E field excitation normal to the CSRRs axis), constructively add-up when CSRRs are placed in such configuration, although the crosscoupling between concentric rings will have an influence on the overall filtering behavior.

To investigate the capability of the proposed concept for noise mitigation in high-speed PCBs boards, a source of switching noise was placed within the parallel-plate PCB, and concentrically surrounded with a set of four CSRR resonators (see Fig. 5(b)). The board is of size 70mm X 60mm, with a Rogers substrate duroid 6010LM. The numerical simulations were carried out using the full-wave finite-element simulator Ansoft HFSS. Transmission coefficient,  $S_{12}$ , is computed, with an observation point placed 4cm away from the source of switching noise, and concentrically surrounded by a set of CSRR resonators in order to effectively isolate the sources of switching noise. For comparison purposes, a solid (reference) board is also considered. The dimensions of the CSRRs resonators were initially characterized in order to estimate their bandgap regions. The radii of the designed CSRRs (see Fig. 5(b)) are  $rin1=4.2\text{mm}$ ,  $rin2=5.0\text{mm}$ ,  $rin3=6.5\text{mm}$ ,  $rin4=6.9\text{mm}$ ,  $rin5=8.2\text{mm}$ ,  $rin6=8.4\text{mm}$ , and outer radius  $rout=10.4\text{mm}$ . The etched copper of the CSRRs is 0.2mm and the spacing between each two concentric edge-coupled CSRR rings is 0.2mm.

Fig. 6(a) shows the transmission coefficient,  $S_{12}$ , for the printed-circuit board with and without the CSRR resonators.  $S_{12}$  is a measure of the electromagnetic unwanted energy that can be present within the board. The results show a wideband suppression of switching noise below -20 dB, covering a wide frequency band

from sub-GHz to almost 10 GHz and beyond. It is interesting to observe that such high band of suppression was achieved with only few resonators at the input and output ports. The strength of the CSRR topology becomes more apparent when the eye diagram for a typical signal transmission above the board is analyzed. Signal integrity is typically analyzed using the eye diagram which gives a measure of distortion in the pulse transmission due to effects of non-ideal reference plane or other parasitic effects that might encounter the signal such as routing through vias. Fig. 6(b) shows the eye diagram for a typical microstrip line stretching over all concentric CSRRs. (The eye diagram was generated using a pseudorandom binary sequence with a pulse width of 1.5ns and 1 volt swing, and nominal rise/fall time is 250ps.) The eye patterns are generated using CST Microwave Studio. In conclusion, not only did the CSRR provide wideband suppression of switching noise, but maintained good signal integrity due to minimal copper etching from the reference board.

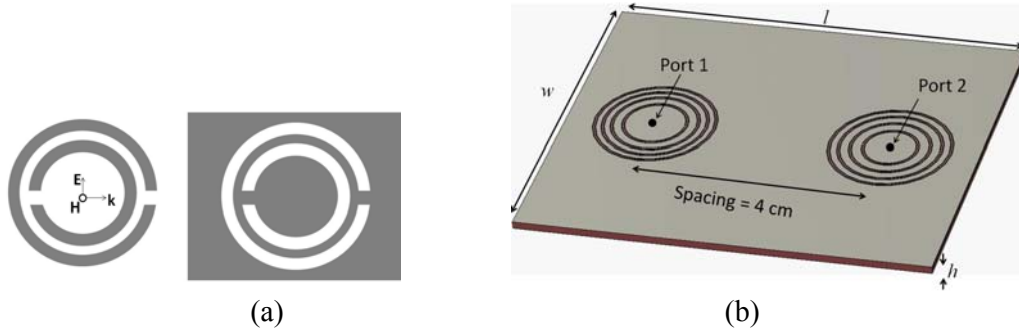


Fig. 5. (a) Split ring resonator and its complementary version. (b) Concentric complementary split ring resonators surround the input and output ports in order to filter undesired switching noise within the power plane.

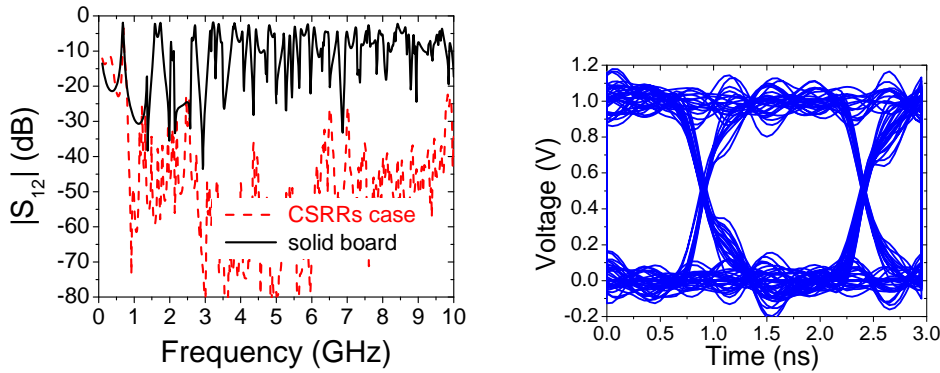


Fig. 6. (a) Magnitude of  $S_{12}$  for the board with and without the CSRRs. (b) Eye diagram for a typical trace extending above the board populated with the CSRR.

## V. Metamaterial for Non-invasive Detection and Microwave sensing

Microwave near-field probes are used to sense the variation of material properties in their close proximity. Due to the fast decaying behavior of near fields, the application of near-field probes is limited to surface or near-surface characterization (Tabib-Azar, 1999), (Qaddoumi, 2006). While increasing the size of the probe allows for deeper penetration into the surface to be detected, the probe resolution will be compromised significantly. In this work, the objective is to increase the sensitivity of the nearfield probe while not compromising its resolution.

Evanescent field amplification, along with the concept of superlensing effect, was proposed by Pendry as a unique property of double (DNG) and single (SNG) negative media, two variants of metamaterials (Pendry, 2000). The superlensing effect was experimentally observed as an indirect proof of the amplification of evanescent waves by DNG and SNG media (Fang, 2003), (Aydin, 2007). In (Boybay, 2008) and (Boybay, 2009), a sensitivity analysis for near-field probes was introduced and furthermore, it was demonstrated analytically that DNG or SNG media when inserted between a source of evanescent waves and the surface to be detected leads to an enhancement of the sensitivity. By using numerical experiments, we show that when a layer of SNG medium is added to the opening of a rectangular waveguide, used as a near-field probe, a significant

enhancement of the probe sensitivity is achieved while at the same time increasing the image quality. As a practical example, we focus on detecting precursor pitting in aluminium plates using a WR-28 waveguide probe. However, the technique presented here can be applied to all types of probes that are based on near-field detection modalities.

Evanescent field amplification can be achieved by both DNG and SNG materials. Since the SNG metamaterials are easier to fabricate and the electromagnetic loss is smaller, SNG materials are used for the amplification in this work. The SNG metamaterials can be designed using SRR inclusions. The evanescent field amplification property of SNG materials depends on the polarization of the field. The epsilon-negative SNG materials amplify TM modes and the mu-negative SNG materials amplify TE modes. The reader is referred to (Pendry, 2000) for a more detailed explanation of the amplification process.

Since the dominant mode in the waveguide is TE<sub>10</sub> mode, a  $\mu$ -negative material is used in this study. For this particular problem, a WR-28 type waveguide is used as the probe since it has been used for crack detection on aluminum plates (Ghasr, 2005). The waveguide has a cross section of 7.11 mm  $\times$  3.56 mm and is operated at 30 GHz. Two other important parameters are the thickness of the SNG layer and the standoff distance, which is defined as the distance between the end of the probe and the aluminum plate. In a conventional probe, without any SNG layer, as the standoff distance increases, the sensitivity decreases. Therefore, as long as the standoff distance is small enough, it is not considered a crucial parameter when there is no SNG layer. On the other hand, when an SNG layer is employed, the standoff distance plays an important role in the optimization process. Fig. 7 shows a schematic of the waveguide probe positioned above a 3 mm thick aluminum plate having a crack. The crack is detected by moving the probe in x-y plane and recording the phase shift in the reflection coefficient.

First, we consider an aluminum plate without any crack to study the phase of the reflection coefficient as a function of the standoff distance for different SNG thicknesses. Fig. 8 shows the phase change as a function of the standoff distance. When there is no SNG layer, the reflection phase has an almost linear variation with respect to the standoff distance. The highest slope is achieved with 0.9 mm SNG thickness. From Fig. 8, when there is no SNG layer, the maximum phase shift due to the target is 0.73°. When an SNG layer is inserted with a standoff distance of 1.1mm and an SNG layer thickness of 0.9mm, the phase shift jumps dramatically to 27°.

To visualize the sensitivity improvement, two-dimensional images were generated by moving the probe along the x and y axes. At each probe position, the reflection phase is recorded and a colormap is generated. The minimum reflection phase is subtracted from the other values to set the minimum reflection phase level to zero. Fig. 9 shows four images generated by four different probe systems. All images are scaled with the same colormap to show the advantage of using the SNG layer and optimizing the standoff distance. In addition to the sensitivity improvement, the image quality is also analyzed. Fig. 9 shows images generated by a probe without SNG layer and a probe with 1.5 mm SNG layer. When there is no SNG layer, the image has side lobes with a magnitude close to half of the center lobe. On the other hand, the SNG layer produces a clear image without side lobes. Therefore the SNG layer improves both the sensitivity and the image quality. As a conclusion, the sensitivity enhancement is a direct consequence of the evanescent field amplification property of SNG media.

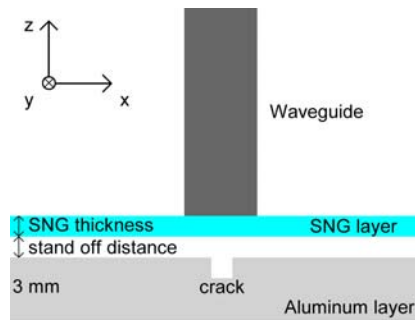


Fig. 7. Schematic showing side view of the waveguide probe positioned on top of the aluminum plate having a crack. The SNG layer covers an area that extends 15 mm in x and y directions from the edge of the waveguide opening (a total area of 33.56 mm by 37.11 mm).

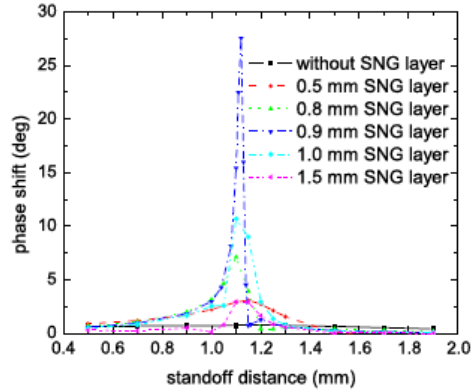


Fig. 8. Phase shift due to the target as a function of the standoff distance.

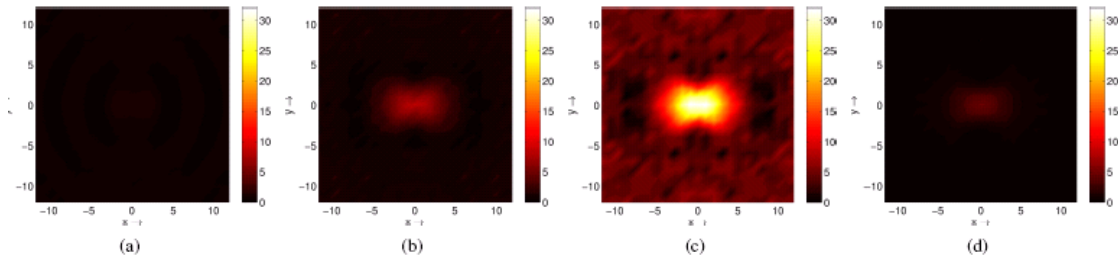


Fig. 9. The image of the 1 mm crack generated by scanning the waveguide in the x-y plane, (a) without SNG layer (b) with 0.8 mm SNG layer (c) with 0.9 mm SNG layer and (d) 1.5 mm SNG layer. The standoff distance is 1.12 mm for (c) and 1.1 mm for the other images. The unit of the axes labels is mm and the unit of the colormap is degree.

## VI. Conclusions

In this paper, we have focused on key applications related to wireless communications. We have shown that metamaterials with its variants such as double negative media, single negative media, and artificial magnetic media can address some very fundamental bottlenecks and challenges, from enhancing the gain and efficiency of low profile antennas, significantly curtailing coupling between high-profile antennas used in MIMO system, to suppressing switching noise which causes false switching in high speed circuits. We also demonstrated that metamaterials can complement the functionality of near-field probes allowing them to provide higher resolution images and increased sensitivity. All this demonstrates that metamaterials not only makes possible uncommon physical phenomena, which are mostly interesting from pure theoretical and academic perspective, but indeed has strong relevance to practical engineering applications.

## References

- Attia, H., and Ramahi, O. M., (2008), "EBG Superstrate for Gain and Bandwidth Enhancement of Microstrip Array Antennas," *Proceeding of IEEE Antennas and Propagation Society International Symposium*, pp. 1 – 4.
- Aydin, K., Bulu, I., and Ozbay, E., (2007), "Subwavelength resolution with a negative-index metamaterial superlens," *Apply. Phys. Lett.*, vol. 90, p. 254102.
- Bhattacharyya, B., (1963), "Input resistances of horizontal electric and vertical magnetic dipoles over a homogeneous ground," *IEEE Trans. Antennas Propag.*, vol. 11, no. 3, pp. 261–266.
- Boybay, M.S, and Ramahi, O.M., (2008), "Near-field probes using double and single negative media," in *Proc. of the NATO Advanced Research Workshop: Metamaterials for Secure Information and Communication Technologies*, Marrakesh, Morocco, pp. 725–731.

- Boybay, M. S., and Ramahi, O. M., (2009), "Near-field probes using double and single negative media," *Phys. Rev. E*, vol. 79, p. 016602.
- Boybay, M.S., and Ramahi, O. M., (2009), "Experimental verification of sensitivity improvement in near field probes using single negative metamaterials," in *Microwave Symposium Digest, 2009 IEEE MTT-S International*.
- Chen, S.-C. Wang, Y.-S., and Chung, S.-J., (2008), "A decoupling technique for increasing the port isolation between two strongly coupled antennas," *IEEE Trans. Antennas Propag.*, vol. 56, no. 12, pp. 3650–3658.
- Choi, J., Govind, V., Swaminathan, M., Wan, L., and Doraiswami, R., (2004), "Isolation in mixed-signal systems using a novel electromagnetic bandgap (EBG) structure," in Proc. IEEE 13th Top. Meet. Electr. Perform. Electron. Packag., Portland, OR, pp. 199–202.
- Dossche, S. , Blanch, S., and Romeu, J., (2005), "Three different ways to decorrelate two closely spaced monopoles for MIMO applications," in *2005 IEEE/ACES International Conference on Wireless Communications and Applied Computational Electromagnetics*, pp. 849–852.
- Falcone, F., Lopetegi, T., Laso, M. A. G., Baena, J. D., Bonache, J., Beruete, M., Marqués, R., Martín, F., and Sorolla, S., (2004), "Babinet principle applied to the design of metasurfaces and metamaterials," *Phys. Rev. Lett.*, vol. 93, no. 19, p. 197401.
- Fang, Z., Liu, T. Yen, and Zhang, X., (2003), "Regenerating evanescent waves from a silver superlens," *Opt. Express*, vol. 11, pp. 682–687.
- Ghasr, M. T., Kharkovsky, S, Zoughi, R., and Austin, R., (2005), "Comparison of near-field millimeter-wave probes for detecting corrosion precursor pitting under paint," *IEEE Trans. Instrum. Meas.*, vol. 54, pp. 1497–1504.
- Jackson, D. R., and Alexopoulos, N. G., (2008), "Gain Enhancement Methods for Printed Circuit Antennas," *IEEE Trans. Antennas Propagation*, vol. AP-33, no. 9, pp. 976-987.
- Kamgaing, T., and Ramahi, O. M., (2003), "A novel power plane with integrated simultaneous switching noise mitigation capability using high impedance surface," *Microwave and Wireless Components Letters, IEEE*, vol. 13, no. 1, pp. 21–23.
- Lee, Y. Ju , Yeo, J., Mittra, R., and Sang Park, W., (2005), "Application of Electromagnetic Bandgap (EBG) Superstrates With Controllable Defects for a Class of Patch Antennas as Spatial Angular Filters," *IEEE Trans. Antennas Propagation*, vol. 53, no. 1, pp. 224-235.
- Pendry, J., (2000), "Negative refraction makes perfect lens," *Phys. Rev. Lett.*, vol. 85, pp. 3966–3969.
- Qaddoumi, N. N., Abou-Khousa, M., and Saleh, W. M., (2006), "Near-field microwave imaging utilizing tapered rectangular waveguides," *IEEE Trans. Instrum. Meas.*, vol. 55, pp. 1752–1756.
- Shahparnia, S., and Ramahi, O. M., (2004), "Electromagnetic interference (EMI) reduction from printed circuit boards (PCB) using electromagnetic bandgap structures," *IEEE Trans. Electromagn. Compat.*, vol. 46, no. 4, pp. 580–587.
- Tabib-Azar, M., Pathak, P. S. , Ponchak, G, and LeClair, S., (1999), "Nondestructive superresolution imaging of defects and nonuniformities in metals, semiconductors, dielectrics, composites, and plants using evanescent microwaves," *Rev. Sci. Instrum.*, vol. 70, pp. 2783–2792.
- Vaughan, R., and Andersen, J., (1987), "Antenna diversity in mobile communications," *IEEE Transactions on Vehicular Technology*, vol. 36, no. 4, pp. 149– 172.